Vol. 04, Iss. 3 (2026) 297-306, DOI: 10.61552/JME.2026.03.001

Journal of Materials and Engineering

www.jme.aspur.rs

Research article

Effects of Surface Roughness, Load and Sliding Speed on the Tribological Behavior of Dry Rubber–Granite Contacts

Ionut Marius Nazarie[a,*], Ilie Musca[a], Ionut Cristian Romanu[a], Irina Besliu-Bancescu[a]

[a]*University „Stefan cel Mare" Suceava, Romania.*

Keywords:

Dry friction
Rubber
Granite
Surface roughness
Sliding velocity

* Corresponding author:

Ionut Marius Nazarie
E-mail : ionut.nazarie@gmail.com

Received: 20 April 2026
Revised: 21 May 2026
Accepted: 23 June 2026

A B S T R A C T

This study investigates dry rubber–granite sliding contact under low normal loads and low sliding speeds. Friction coefficients were measured using an MFT2000 tribometer for three normal load levels and ten sliding speeds, considering two different surface roughness conditions. Surface microtopography was characterized using MarSurf CM 3D optical microscopy. The results demonstrate that surface microtopography plays a dominant role in this regime, leading to relatively high friction coefficient values. The friction response is governed by the coupled effects of normal load, sliding velocity, and roughness characteristics. An increase in sliding speed results in higher friction coefficients, followed by a tendency toward stabilization at higher velocities. A quantitative analysis of the experimental data, based on the standard deviation of repeated measurements, reveals an increasing dispersion of friction values with both load and speed. This behavior highlights the growing influence of viscoelastic deformation and micro-asperity interactions and indicates a transition from adhesion-dominated contact at low speeds to a regime increasingly controlled by hysteresis effects. The study provides an interpretation of friction mechanisms in low-speed elastomeric contacts, contributing to a better understanding of rubber–surface interaction under dry conditions.

© 2026 Journal of Materials and Engineering

1. INTRODUCTION

During the landing and take-off procedures of aircraft on an airport runway, the quality and friction characteristics of the runway surface play an essential role in ensuring flight safety [1].

For a clearer understanding of the interaction between tires and the runway, laboratory simulations were performed under conditions close to reality.

Thus, the rubber-granite contact was analyzed for different roughness, sliding, rolling and

combined rolling with sliding motion, at different loads, different surface contaminations and measurement speeds. This study deals with the sliding behavior in rubber-granite contact, dry surface at low measuring speeds.

Granite is a rock frequently found as an aggregate in asphalt or concrete mixtures used in the construction of automobile roads, highways or airport runways. To study the effect of this component on the friction between the tire and the runway, a series of friction experiments were carried out between granite slabs and a semi-spherical pin made of airplane tire rubber.

2. THEORETICAL CONSIDERATIONS

The theory of rubber friction, developed by Kummer and Geyer [2], considers that the value of the total friction force, F_T, is:

$$F_T = F_A + F_H + F_V + F_C \quad (1)$$

where F_A – adhesion force; F_H – hysteresis force; F_V – shear forces of a viscous liquid layer between the elastomer and the surface; F_C - intramolecular cohesion forces.

Due to large difference between the elastic and viscous characteristics of the two materials used: rubber and granite, friction in this situation presents distinct particularities because the stiffness of the two materials are very different and thus granite can be considered absolutely rigid compared to rubber.

In contact, due to the differences and incompatibility at the molecular level between granite and rubber, the cohesion is not significant. Thus, having reference equation (1), for the analysis, in the case of contact on a dry surface it is observed that the value of the total friction force in the coupling becomes:

$$F_T = F_A + F_H \quad (2)$$

On microcontacts an adhesive contact will appear, which in the presence of movement will generate tangential adhesion forces.

In reality, the hysteresis phenomenon (correlated with the elastic deformations of the rubber) and the adhesion phenomenon (correlated with the contact area) overlap, the variations of the friction coefficient in the coupling being a superposition of the two variations.

In other formulation, Tiwari et all [3], for dry rubber-granite contact, the total friction force may therefore be interpreted as the sum of an adhesion term and a hysteresis term:

$$F_f = \tau \cdot A_r + F_H \quad (3)$$

where τ is the interfacial shear strength, A_r is the real contact area, and F_H is the hysteresis contribution associated with viscoelastic energy dissipation in the rubber during cyclic deformation over surface asperities.

At low speed, the rubber has sufficient time to conform to the granite asperities, which increases A_r and strengthens the adhesive contribution. As sliding speed increases, the deformation frequency of the rubber also increases; consequently, viscoelastic losses become more important and the hysteresis component contributes to the increase of the friction coefficient. This interpretation explains why the measured coefficient of friction depends simultaneously on load, speed and surface microtopography.

3. EXPERIMENTAL METHODOLOGY

To obtain friction coefficients values, the MFT-2000 tribometer was used, which allows multiple configurations. The test programs are fully automated and the advanced controllers allow highly repeatable and accurate measurements, [4].

For data interpretation and to create readable graphs, a measurement number was associated with each measurement speed, table1.

Table 1. Test - speed matrix.

Test No.	Sliding Speed v [m/s]
1	1.05E-06
2	1.05E-05
3	1.05E-04
4	1.05E-03
5	5.00E-02
6	5.24E-02
7	7.85E-02
8	1.05E-01
9	1.57E-01
10	2.09E-01

The experiments were conducted applying constant normal forces (Fn) of 1 N, 3 N and 5 N using the tribometer, ensuring a constant normal load throughout the experiments with no relative motion in the contact zone during loading.

The graphical representations were not made by points, although the friction coefficient values are discrete.

In order to show the trend of the values of friction coefficient and its behavior depending on the conditions in the analyzed contact it were use lines.

The rubber used for the test is part of a Goodyear-Flight Special II, 6.00-6 aircraft tire and was shaped into a spherical surface with a diameter of approximately 8 mm.

The rubber in the tire is mainly of the RSS1 (Ribbed Smoked Sheets) type, a natural rubber with high purity, relatively high coefficient of friction, superior elasticity and durability.

Before the measurements were made, the contact surfaces, granite and rubber, were cleaned to remove any impurities from the materials that could influence the results. The surface was cleaned using a solvent, rinsing with deionized water, and drying with filtered compressed air.

For the characterization of the microtopography, figure 1, the test surfaces, white granite plate, a MarSurf CM - 3D Optical Microscopy [5], equipment was used. Following the analysis of the roughness parameters, determined according to the ISO 4287 standard, it results that surface 2 is rougher than surface 1.

Surface 1 can be considered more uniform and smoother, with a more homogeneous distribution of asperities, whereas surface 2 is rougher, characterized by a more pronounced topography, with higher peaks and deeper valleys, which gives it a more pronounced functional character.

The interpretation of the microtopography identified the first surface, figure 1, marked with roughness 1, as a relatively rough surface, presenting more valleys than peaks (yellow-green color).

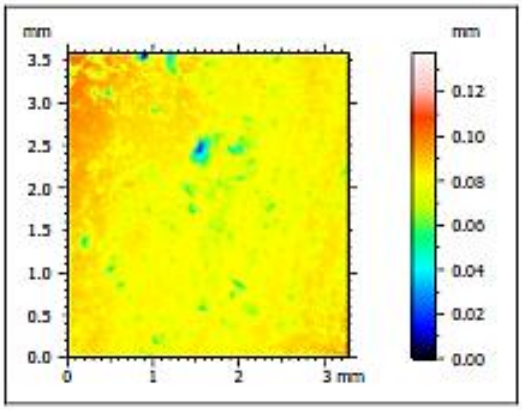


Fig. 1. 3D topography of the granite surface during sliding roughness 1.

In the case of the second surface, figure 2, marked with roughness 2, the distribution is higher for peaks (red areas).

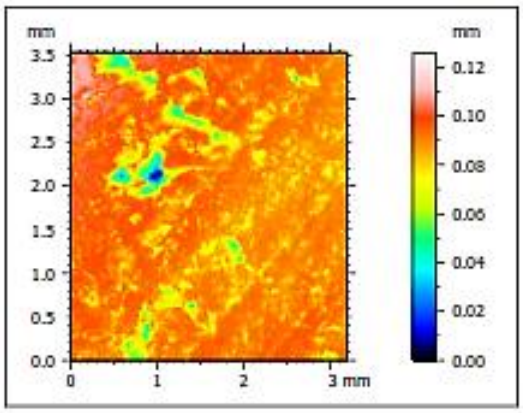


Fig. 2. 3D topography of the granite surface during sliding roughness 2.

Following the analysis of surface roughness parameters, the topographical maps shown in fig.1,2 provide a visual representation of the surface morphology corresponding to the measured parameters, table 2.

Table 2. Surfaces roughness parameters.

Surface	Sa [µm]	Ssk
Roughness 1	4,882	-1,386
Roughness 2	32,500	-0,494

The first surface (roughness 1) , characterized by Sa=4.882 µm and a strongly negative skewness Ssk=−1.386, exhibits a microtopography dominated by valleys, visible as blue–green regions distributed across the surface. These features are associated with microcracks and pores, leading to a discontinuous but highly interactive contact interface.

In contrast, the second surface (roughness 2) , with Sa=32.5 µm and Ssk=−0.494, presents a more developed roughness amplitude, with a larger proportion of elevated regions (yellow–red zones), indicating increased asperity height and a more continuous load-bearing structure.

From a tribological perspective, these differences in surface morphology directly influence friction behavior. The valley-dominated surface (roughness 1) promotes localized deformation and mechanical interlocking of the rubber, increasing the real contact area and enhancing adhesion-controlled friction at low speeds.

To approximate the real contact area the Fujifilm Prescale film, pressure sensitivity range of 0.05–0.2 MPa at the interface between the spherical rubber specimen and the rigid granite surface, was loaded using the MFT-2000 tribometer by imposing only a normal approach between the rubber specimen and the granite surface, without relative motion in the contact zone. The applied normal loads were 1 N, 3 N and 5 N, fig.3.

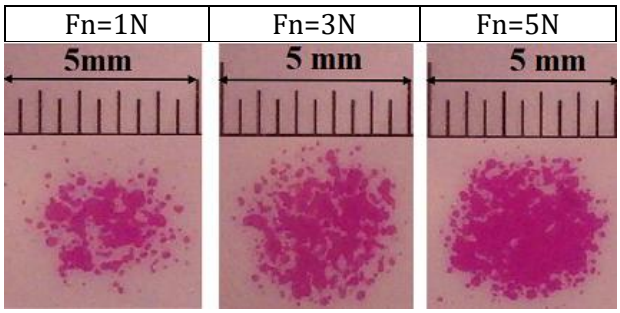


Fig. 3. Static contact area of the rubber specimen.

At the lowest normal load, only a reduced number of asperities are in contact with the rubber specimen. As the load increases, the contact zone expands, the contact boundary becomes clearer and the density of active micro-asperity contacts increases. The apparent contact area has an approximately circular shape, consistent with the geometry of the rubber specimen.

To approximate the real contact area, the images were processed using Fiji/ImageJ by applying color thresholding in order to separate the red contact regions from the background and convert the image into a binary map. The software calculates the total contact area by identifying the pixels associated with the segmented contact spots, summing their projected surface, and converting the pixel-based area into physical units using the calibrated spatial scale. Morphological filtering operations were additionally applied to reduce image noise, eliminate isolated pixels, and improve the continuity of the detected contact regions before the final area computation

The contact images, using this software, are shown in fig. 4, which indicate that the contact occurs mainly on micro-asperities.

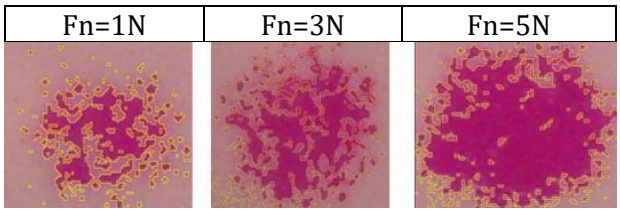


Fig. 4. The contact images for normal load of 1 N, 3 N and 5 N using Fiji/ImageJ.

The contact images presented in Fig. 4 indicate that the contact occurs mainly on micro-asperities and progressively expands with increasing normal load. The apparent contact area was approximated by a circular geometry corresponding to the overall contact contour, while the real contact area was determined as the cumulative area of the segmented red pixel regions representing the effective micro-contact spots. The contact efficiency was subsequently evaluated as the ratio between the real contact area obtained from pixel analysis and the apparent circular contact area.

The obtained ratios between real and apparent contact area were 78.85% for 1 N, 83.81% for 3 N and 85.32% for 5 N. These values show that the real contact area increases with normal load, fig.4, confirming the progressive engagement of surface asperities and the increasing contribution of adhesion to the total friction force. The increase in real contact area with load confirms the viscoelastic compliance of rubber and its ability to conform to the surface microtopography, real contact area increases slowly with normal load, which is consistent with elastomer contact behavior at low loads. This behavior supports the experimentally observed decrease of the friction coefficient with increasing load, as the increase in real contact area is not proportional to the increase in normal force, fig. 5.

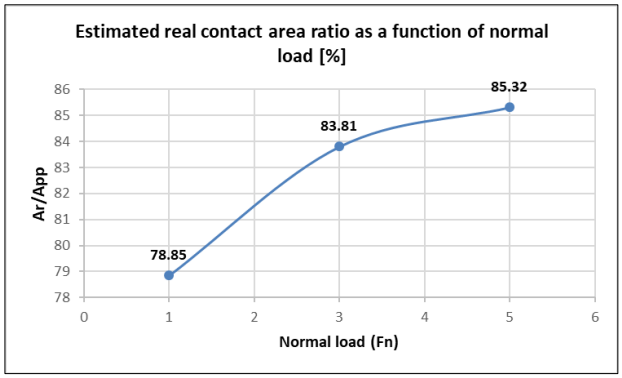


Fig. 5. Estimated real contact area ratio as a function of normal load.

The increase in A_r with Fn is consistent with elastomer contacts mechanics.

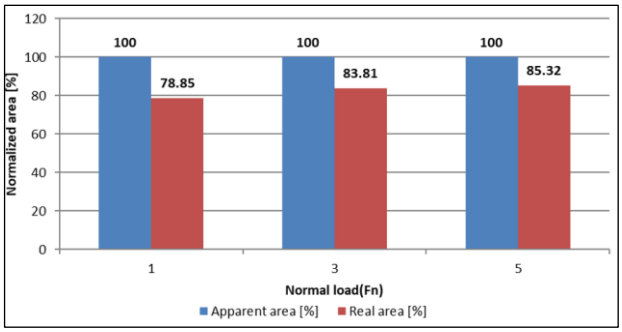


Fig. 6. Normalized comparison between apparent and real contact area.

In fig. 6, the trend reflects the progressive activation of micro-asperities and indicating progressive engagement of micro-asperities and improved conformity of the rubber to the granite surface, although full contact is not achieved due to the inherently discrete nature of surface interactions.

4. EXPERIMENTAL RESULTS AND DATA INTERPRETATION

The following section presents the results obtained from the experimental tribological measurements. An initial qualitative evaluation of the evolution of the friction coefficient as a function of the investigated operating parameters is first discussed, followed by a quantitative statistical analysis and interpretation of the measured data.

The figure 7, shows the evolution of the friction coefficient, in dry contact, Fn= 5N, for the 10 measurement speeds, roughness 1.

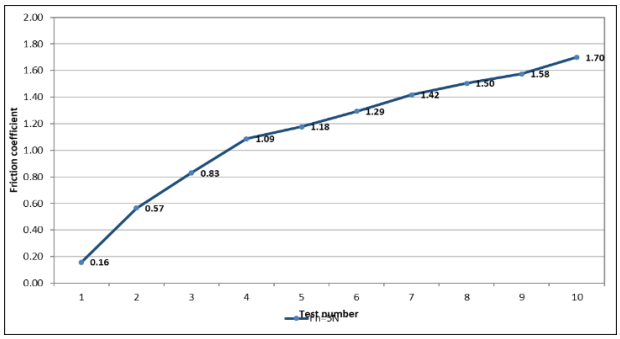


Fig. 7. Friction coefficient between rubber and granite, dry contact, Fn - 5N, roughness 1.

It is observed that the values of the friction coefficient, at a constant load, in our case Fn=5N, increase as the measurement speed increases.

In the following figure a comparative analysis is performed for the friction coefficient measured values at the lowest (test 1) and highest (test 2) measurement speeds. The values of speed were chosen to highlight differences in the friction coefficient depending on the measurement speed.

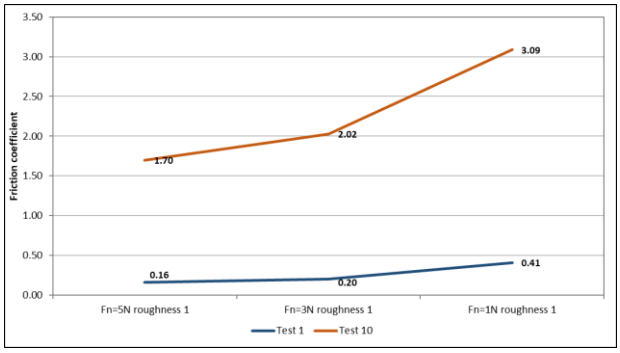


Fig. 8. Friction coefficient, roughness 1, test no.1 and no. 10.

Figure 8 presents the trend of the friction for test 1 and test 10, for the values of the force Fn=1N, 3N, 5N, in the case of roughness 1.

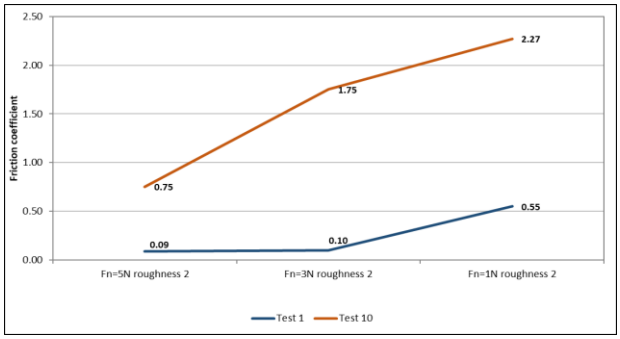


Fig. 9. Friction coefficient, roughness 2, test no.1 and test no.10.

Figure 9 presents the trend of the friction for test 1 and test 10, for the values of the force Fn=1N, 3N , 5N in the case of roughness 2.

As can be seen in these separate analyses, figure 8 and figure 9, the coefficient tends to increase with increasing measurement speed.

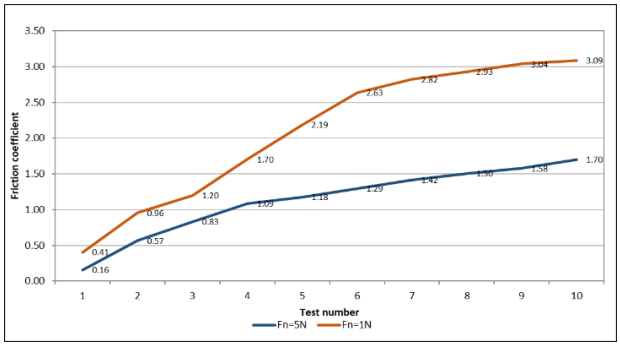


Fig. 10. Friction coefficient between rubber and granite, dry contact, Fn- 5N and 1N, roughness 1.

Figure 10 shows a graph comparing the values of the friction coefficient for the values of Fn=5N and Fn=1N, in the 10 measurement speeds, on the surface of roughness 1.

In this particular case it is observed that an increase in load leads to a decrease in the values of coefficient. An increase in load reduces the friction coefficient between a rubber and granite contact at low speeds because a higher load increases the true contact area more than proportionally, leading to a greater contribution from adhesion and hysteresis at the micro-scale, despite the total surface area remaining constant. This phenomenon is due to the rubber deforming to fill the granite's surface irregularities, resulting in a larger actual contact area and consequently a higher friction force for a given load, which effectively lowers the friction coefficient.

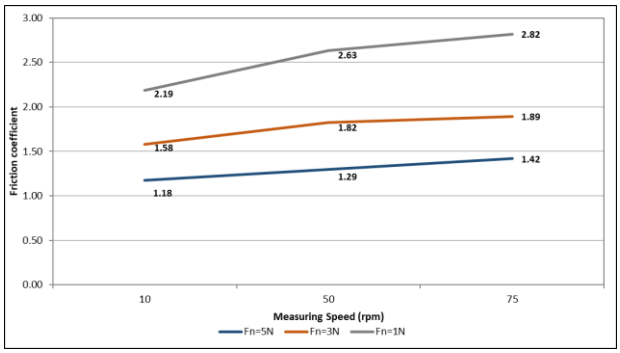


Fig. 11. Friction coefficient between rubber and granite, dry contact, Fn- 1N, 3N, 5N, roughness 1, related to measuring speed.

In order to analyze the influence of the measurement speed on the values of the friction coefficient in the following graphs, fig. 11 and fig. 12, a comparative analysis is performed for its evolution on the two roughnesses, at the same measurement speeds (10, 50, 75 rpm) and the same contact load (Fn= 1N, 3N, 5N).

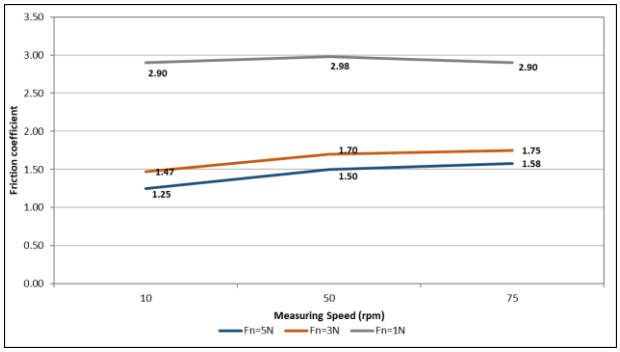


Fig. 12. Friction coefficient between rubber and granite, dry contact, Fn- 1N, 3N, 5N, roughness 2, related to measuring speed.

In both representations, for the two roughness, it is observed that the value of the friction coefficient tends to increase with increasing measurement speed at similar loads.

It is observed that in dry contact, as the speed increases, the friction coefficient also increases. This is due to the characteristics of the rubber used, the relative speed and the microtopography of the surface.

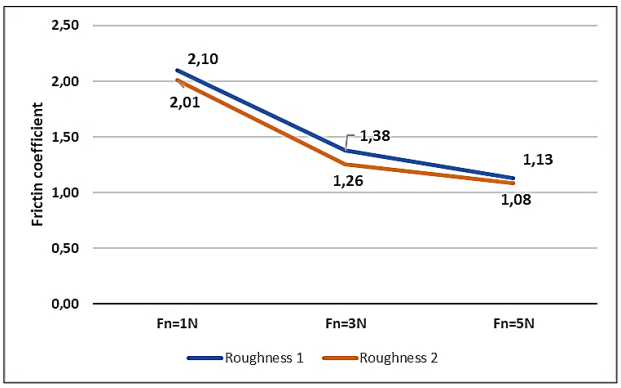


Fig. 13. Mean values of friction coefficients depending on roughness.

In dry contact between rubber and granite [6], with a constant normal force and a variation in the tangential force, the friction coefficient between rubber and granite increases because: RSS1 type rubber is a hyperelastic material,

which deforms to adapt to the micro-asperities of the granite surface; at low speeds, the rubber has time to deform and penetrate deeper into the asperities of the granite, which increases the effective contact surface and, implicitly, the friction; at low speeds, the contact time between rubber and granite is sufficient to allow the formation of stronger adhesive bonds between the contacting bodies.

The figure 13 shows a comparative representation of the mean values of the friction coefficients as a function of the contact load.

As in the previous cases, it is observed that in the case of roughness 1, the friction coefficient values are higher than in the case of roughness 2, this aspect being determined mainly by the microtopography of the test surface and the type of rubber used.

The quantitative comparison should be interpreted together with the measurement dispersion. The increase of scatter with load and speed suggests that the contact becomes more sensitive to local micro-slip, asperity deformation and non-uniform growth of the real contact area.

From this point of view, the friction coefficient is governed by two coupled effects: the adhesive term, controlled by the real contact area, and the hysteresis term, controlled by the viscoelastic deformation of rubber over the granite microtopography. The observed trends are consistent with this combined mechanism rather than with a purely descriptive dependence on speed or load.

Statistical analisys

For repeatability, each experimental condition was repeated three times under the same normal load, sliding speed and surface roughness conditions. The values presented in the graphs correspond to mean values obtained from repeated measurements.

The dispersion of the measured friction coefficient was evaluated using the sample standard deviation [7]:

$$\sigma = \sqrt{\frac{1}{n-1} \cdot \sum_{i=1}^{n} (x_i - \bar{x})^2} \qquad (4)$$

Here, x_i is an individual measured friction coefficient, $\bar{x}$ is the arithmetic mean, and n is the number of values used in the calculation. For each normal load, n = 10 because the ten test values are used. For test-by-test dispersion, n = 3 because the values for Fn = 1 N, 3 N and 5 N are compared at the same test number.

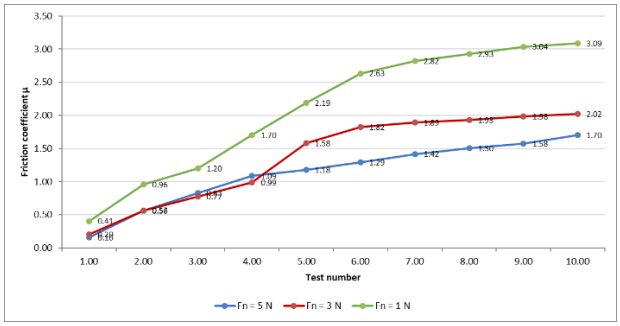


Fig. 14. Friction coefficient vs test number.

At low test numbers, corresponding to low sliding speeds, fig. 14, the friction coefficient values obtained for different normal loads are relatively close. This indicates a comparatively stable contact regime, where the rubber specimen interacts with the granite surface mainly through a limited number of micro-asperity contacts.

In this initial regime, the adhesion component is expected to dominate because the rubber has sufficient time to conform locally to surface asperities and to develop interfacial contact without strong dynamic excitation.

As the speed increases, the separation between the curves becomes more pronounced. This shows that the friction response becomes increasingly dependent on normal load and sliding speed. The larger differences between the 1 N, 3 N and 5 N curves indicate that the contact no longer behaves as a simple load-independent interface.

At higher test numbers, the higher friction values and the larger separation between curves suggest an increased contribution of viscoelastic energy dissipation. Therefore, the trend supports a transition from an adhesion-controlled regime toward a hysteresis-dominated regime, where rubber deformation and recovery over granite asperities become more important.

In fig. 15, the standard deviation calculated for each normal load quantifies the dispersion of

the ten friction-coefficient values obtained over the test sequence. In this analysis, sigma is not only a statistical quantity, but also an indicator of how sensitive the contact response is to the imposed test conditions.

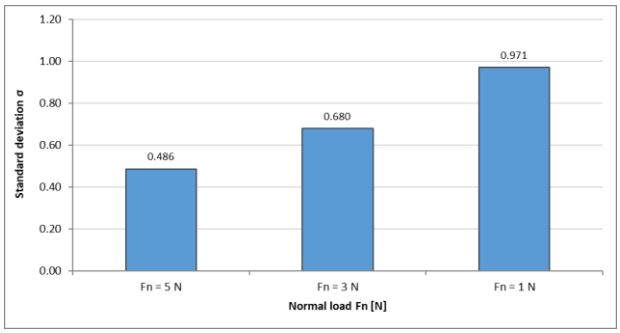


Fig. 15 Standard deviation σ by normal load.

The increase of sigma with normal load shows that the variability of friction measurements becomes larger as the applied load increases. At higher load, the rubber penetrates more deeply into the surface microtopography and engages a larger number of asperities.

This produces a more complex and heterogeneous contact configuration. Local variations in asperity height, rubber deformation and micro-slip can therefore generate larger fluctuations in the measured friction coefficient.

Consequently, the figure supports the conclusion that increasing normal load enhances the sensitivity of rubber-granite contact to deformation and micro-asperity interaction.

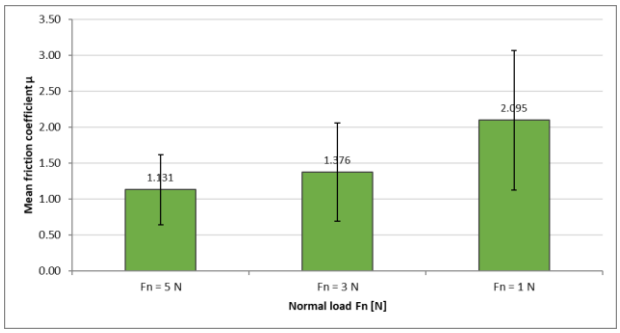


Fig. 16. Mean friction coefficient with ±σ error bars.

Figure 16 represent the mean friction coefficient calculated for each normal load, while the vertical error bars represent the corresponding sample standard deviation. This representation directly addresses the repeatability and dispersion of the experimental results.

The error bars provide a quantitative validation of the measured trends. Smaller error bars indicate a more repeatable response, whereas larger error bars reveal stronger variability of the contact conditions during the sequence of tests.

The observed dispersion confirms that friction in rubber-granite contact is affected by coupled mechanisms, including real contact area evolution, micro-asperity engagement and viscoelastic deformation of the rubber.

The use of mean values together with ±sigma therefore improves the reliability of the interpretation, because the trends are no longer presented only qualitatively but are supported by statistical information.

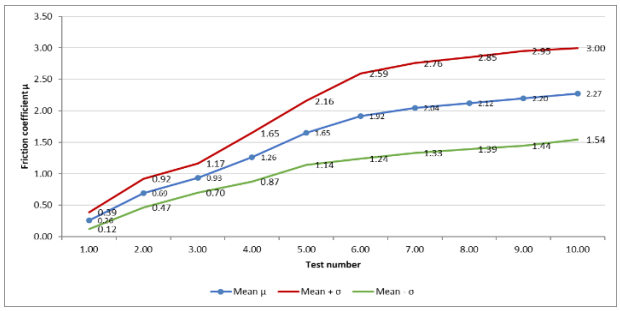


Fig. 17 Mean friction coefficient with ± σ envelope as a function of test number.

In fig. 17, the envelope defined by mean μ ± sigma shows how the overall dispersion of the friction coefficient evolves during the test sequence. At the beginning of the tests, the envelope is relatively narrow, indicating a stable friction response with limited variability between normal loads.

As the test number increases, the envelope widens. This means that the friction response becomes more sensitive to the combination of load and sliding condition. The widening of the envelope is consistent with a progressive increase in viscoelastic deformation effects.

This representation is useful because it combines the mean friction trend with the associated uncertainty interval. It therefore gives a clearer picture of the stability of the tribological response than a simple mean curve.

The evolution of the envelope supports the interpretation that the rubber-granite contact

shifts from a relatively stable adhesion-controlled regime at low speeds toward a more complex regime dominated by hysteresis and internal damping at higher speeds.

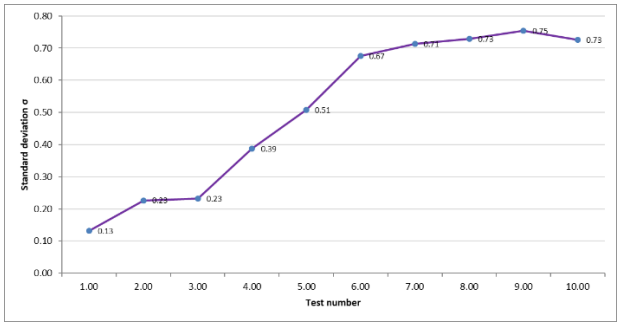


Fig. 18. Standard deviation σ at each test.

The figure 18 shows the standard deviation calculated at each test number using the three friction-coefficient values corresponding to Fn = 1 N, 3 N and 5 N. Therefore, the curve describes how the spread of the friction response between loads evolves from one test condition to another.

At low test numbers, sigma has small values. This indicates that the friction coefficients measured under different normal loads are relatively close, which suggests stable and uniform contact conditions. In this range, the influence of normal load is limited and the contact is mainly governed by adhesion at micro-asperity level.

As the test number increases, sigma rises significantly. This growth indicates that the friction coefficient becomes increasingly dependent on normal load. The stronger separation between load cases reflects the increasing contribution of rubber deformation and viscoelastic losses.

At higher test numbers, sigma reaches larger values, showing that the friction behavior is strongly load-dependent. This confirms that hysteresis effects become dominant in the investigated dry rubber-granite contact, especially when the deformation frequency associated with sliding increases.

Taken together, the figures show that the friction coefficient increases with test number, while the dispersion also increases. This combined trend indicates that the contact becomes progressively more sensitive to load and sliding condition.

The statistical analysis therefore supports the physical interpretation of the experimental results: at low speeds, adhesion and stable microcontact formation dominate, whereas at higher speeds, viscoelastic hysteresis and load-dependent deformation become increasingly important.

5. CONCLUSIONS AND DISCUSSIONS

At low speeds and low normal forces, the surface microtopography plays a main role in the values of the friction coefficient, which is higher. The present study demonstrates that friction behavior in rubber–granite contact at low speeds is primarily governed by the evolution of real contact area and its nonlinear dependence on normal load. The integration of friction measurements with contact area analysis provides a deeper understanding of adhesion-dominated regimes, representing a relevant contribution to tribological studies of elastomeric materials.

The dispersion of the friction coefficient values becomes higher with increasing speed and Fn value. A key novelty of this work consists in establishing a direct experimental correlation between real contact area and friction coefficient in low-speed, low-load dry rubber–granite contact, highlighting the dominant role of micro-asperity interaction and adhesion-controlled mechanisms.

The conclusions resulting from the study, carried out at low speeds and low normal forces, are:

- in sliding motion, dry contact, the values of the friction coefficient are mainly influenced by the load, the contact speed and the microtopography of the surface;
- the friction coefficient increases with the relative contact speed, with a tendency to attenuate at higher speeds;
- the microtopography of the test surface and the type of rubber significantly influence the values of the friction coefficient in the range of forces and measuring speeds used.

For dry contact conditions, as reported in [8], a similar trend in the friction coefficient at low sliding speeds is observed. In our case as well, the friction coefficient increases with increasing speed.

Based on the findings reported by R. Shi et al. [9], surface topography represents an essential parameter of solid structures involved in interface phenomena, having a decisive influence on friction, wear, and lubrication behavior, particularly under mixed lubrication and dry friction conditions. Surface microtopography manifests as a random structure composed of microscopic asperities and cavities (peaks and valleys), generated during manufacturing processes, and constitutes a characteristic commonly encountered in most engineering applications.

The experimental investigations and measurements carried out support the hypothesis regarding the previously mentioned aspects, demonstrating that surface microtopography plays a significant role in contact phenomena. In particular, in rubber–granite contact, the microtopography features of the interacting surfaces act as one of the main influencing factors, having a pronounced effect on the resulting friction coefficient values.

The static contact area measurements performed with Fujifilm Prescale and processed in Fiji/ImageJ showed that the real contact area increased from 78.85% to 85.32% of the apparent area when the normal load increased from 1 N to 5 N. This confirms that the number and density of active microcontacts increase with load.

The combined interpretation of friction coefficient, microtopography and real contact area provides a clearer explanation of the measured behavior. Adhesion is mainly associated with A_r, while hysteresis is associated with the deformation and recovery of rubber around granite asperities during sliding.

The specific contribution of this work is the analysis of dry rubber-granite sliding under low normal loads and very low sliding speeds, combined with the characterization of granite microtopography and the estimation of the static real contact area. The present work focuses on the load-speed range relevant to incipient sliding and micro-asperity contact, where adhesion and hysteresis mechanisms coexist and strongly affect the measured friction coefficient.

Future investigations will include a viscoelastic characterization of the rubber compound in order to separate quantitatively the adhesive and hysteresis components.

REFERENCES

[1] European Union Aviation Safety Agency (EASA), *Easy Access Rules for Aerodromes: Regulation (EU) No. 139/2014, AMC1 ADR.OPS.C.010(b)(3) – Maintenance of Pavements, Other Ground Surfaces and Drainage*, Cologne, Germany, Dec. 2024.

[2] H. W. Kummer, *Unified Theory of Rubber and Tire Friction*, Engineering Research Bulletin, Pennsylvania State University, 1966.

[3] A. Tiwari, N. Miyashita, N. Espallargas, and B. N. J. Persson, "Rubber friction: The contribution from the area of real contact," *The Journal of Chemical Physics*, vol. 148, no. 22, p. 224701, Jun. 2018, doi: 10.1063/1.5037136.

[4] RTec Instruments, *MFT Software User's Manual*, document AS-04A-EN, RTec Instruments, San Jose, CA, USA, 2022.

[5] Willrich Precision Instrument Co., *MarSurf CWM 100 3D Measurement System: Confocal Microscope with Integrated White Light Interferometer*, 2013.

[6] I. M. Nazarie, I. Musca, I. C. Romanu, and I. Besliu-Bancescu, "Experimental study on Rubber-Granite friction in dry and contaminated contact," *Tribology in Industry*, vol. 47, no. 4, pp. 743–752, Dec. 2025, doi: 10.24874/ti.2040.10.25.11.

[7] D. C. Montgomery, *Design and Analysis of Experiments*, 8th ed. New York, NY, USA: John Wiley & Sons, 2013.

[8] L. Busse, I. Boubakri, and M. Klüppel, "Friction master curves for rubber on dry and wet granite," *KGK Kautsch. Gummi Kunstst.*, vol. 64, no. 5, pp. 35–39, 2011.

[9] R. Shi, B. Wang, Z. Yan, Z. Wang, and L. Dong, "Effect of surface topography parameters on friction and wear of random rough surface," *Materials*, vol. 12, no. 17, p. 2762, Aug. 2019, doi: 10.3390/ma12172762.